Molecule condensate production from an atomic Bose-Einstein condensate via Feshbach scattering in an optical lattice: Gap solitons

Richard S. Tasgal,[1] G. Menabde,[1] and Y. B. Band[1,2]
[1]*Departments of Chemistry and Electro-Optics, Ben-Gurion University of the Negev, P.O.B. 653, Beer-Sheva 84105, Israel*
[2]*Atomic Physics Division, A267 Physics, National Institute of Standards and Technology, Gaithersburg, Maryland 20899, USA*
(Received 18 August 2006; published 14 November 2006)

We propose a scheme for making a Bose-Einstein condensate (BEC) of molecules from a BEC of atoms in a strongly confining two-dimensional optical lattice and a weak one-dimensional optical lattice in the third dimension. The stable solutions obtained for the order parameters take the form of a different type of gap soliton, with both atomic and molecular BECs, and also standard gap solitons with only a molecular BEC. The strongly confining dimensions of the lattice stabilize the BEC against inelastic energy transfer in atom-molecule collisions. The solitons with atoms and molecules may be obtained by starting with an atomic BEC, and gradually tuning the resonance by changing the external magnetic-field strength until the desired atom-molecule soliton is obtained. A gap soliton of a BEC of only molecules may be obtained nonadiabatically by starting from an atom-only gap soliton, far from a Feshbach resonance and adjusting the magnetic field to near Feshbach resonance. After a period of time in which the dimer field grows, change the magnetic field such that the detuning is large and negative and Feshbach effects wash out, turn off the optical lattice in phase with the atomic BEC, and turn on an optical lattice in phase with the molecules. The atoms disperse, leaving a gap soliton composed of a molecular BEC. Regarding instabilities in the dimension of the weak optical lattice, the solitons which are comprised of both atoms and molecules are sometimes stable and sometimes unstable—we present numerically obtained results. Gap solitons comprised of only molecules have the same stability properties as the standard gap solitons: stable from frequencies slightly below the middle of the band gap to the top, and unstable below that point. Instabilities are only weakly affected by the soliton velocities, and all instabilities are oscillatory.

DOI: 10.1103/PhysRevA.74.053613 PACS number(s): 03.75.Lm, 03.75.Mn, 05.45.Yv

I. INTRODUCTION

External magnetic fields, and confinement in a strong external potential that can effectively reduce the dimension from three-dimensional (3D) to 2D or 1D, can be used to control atomic interactions in trapped ultracold quantum gases. An example of the former is the tuning of a magnetic field for a system with a diatomic Feshbach resonance [1,2] to convert *fermionic* atoms into weakly bound bosonic molecules (which in some cases were remarkably long-lived) [3]. Magnetic fields have also been used to tune the scattering near a Feshbach resonance for *bosonic* atoms in a Bose-Einstein condensate (BEC) [4–13]. However, a high rate of atom loss exists and, unlike for fermions, only a small fraction of molecules have been observed in the bosonic case. The loss has been attributed to collisional decay of the nascent highly excited vibrationally excited molecular state via inelastic collision processes, e.g., vibrational-to-translational energy transfer [14]. For fermionic atoms this loss mechanism is suppressed due to Pauli blocking [15]. An example of confinement control is the confinement-induced resonances predicted [16] and experimentally observed [17] in a quasi-one-dimensional fermionic atom gas confined in an optical lattice.

Here we propose a scheme for production of molecular BECs in the form of gap solitons. The suggested system has a deep 2D optical lattice (OL) and a relatively shallow periodic optical lattice perpendicular to the deep 2D lattice. There is an external magnetic field with strength such that the atom and dimer BECs have zero (or large) detuning [and, as a consequence, a Feshbach resonance can serve to strongly (weakly) couple atoms to molecules]. The deep 2D OL reduces the effective dimensionality of the dynamics from 3D to 1D, and the shallow 1D lattice perpendicular to it induces band gaps at the edge of the Brillouin zone. Because of the quadratic nature of the Feshbach interaction the frequency and wave vector of the molecular BEC are double those of the atomic BEC. Consequently, for both the atomic and molecular BECs to be in forbidden gaps, the shallow optical lattice should have two spatial frequencies, one in phase with the atomic BEC, and a second with a period shorter by the factor 2, in phase with the dimer BEC.

The optical lattice has a critical role in stabilizing molecular BECs. Confinement of the system to effectively one dimension reduces the inelastic energy transfer collision processes between atoms and molecules which have plagued attempts to create long-lasting molecular BECs. Reduction of collisional loss as a result of confinement in the transverse dimensions is actually a generic property of ultra cold gases [18], and is not unique to the specific model herein. For example, Ref. [19] predicted that the second- and higher-order local correlation functions would vanish in quasi-1D systems, which was strikingly confirmed experimentally in Ref. [20] which reported measurements of the three-body recombination rate for a BEC in a magnetic trap in one dimension (where the 1D behavior of the dynamics is due to application of a strong 2D optical lattice) and found it to be strongly reduced relative to the 3D rate. Several papers have reported molecule production in 3D optical lattices. Reference [21] demonstrated controlled production of molecules

in optical lattices (though with considerable loss). In contrast to the present work, the molecules were created starting from atoms in the Mott insulating phase and a two-photon Raman transition created single molecules on the lattice sites occupied by two atoms. References [22–24] reported production of stable molecules in 3D optical lattices, the first two using ^{87}Rb, and the third producing a heteronuclear molecule from ^{87}Rb and ^{40}K. Damski *et al.* [25] had also considered optical lattices with BECs to create a Mott insulator, and from that further manipulated the atomic BEC to create a dipolar BEC. There has been work on using Feshbach resonances to obtain BECs of molecules from BECs of atoms without any use of solitons [26,27].

In our system, the fact that the molecules sit in the gap has the potential to further reduce inelastic collision processes between atoms and molecules, and between molecules, because of the reduction of phase space for molecules in other vibrational states that could be produced by such deleterious collisions. Moreover, the weak 1D optical lattice allows an additional degree of tuning of the system, providing a useful additional degree of control.

We develop a mean-field (Gross-Pitaevskii) treatment of the system, and analyze the collective dynamics within this framework, where the Feshbach interactions, and the mean-field interactions between atoms, between molecules, and between atoms and molecules are nonlinear. The existence of nonlinear effects opens the possibility of nonlinear structures existing where the linear dispersion relation forbids linear solutions. Numerical analysis of the dynamical equations indeed shows that, over a range of optical lattice and magnetic-field strengths, the system supports two types of gap solitons, i.e., stable nonlinear localized structures within band gaps [28–30]. The solitons here share some similarities with two-component optical gap solitons that were studied in a nonlinear waveguide with a Bragg grating [31]. There are gap solitons made up of both atoms and molecules, and there are gap solitons consisting entirely of molecules. We find a nonadiabatic route by which gap solitons with molecules only can be obtained from an initially purely atomic BEC.

The paper is organized as follows: Section II describes the system under study, presents the mean-field equations for the atomic and molecular BEC and develops the 1D mean-field equations. Section III discusses soliton solutions of these equations and describes the numerical results. Section IV shows how to dynamically prepare the gap solitons from an initial atomic BEC state. Summary and conclusion are in Sec. V.

II. REDUCED DIMENSIONAL OPTICAL LATTICE SYSTEM

We derive the mean-field equations starting from the many-body Hamiltonian for the 3D system with condensed atoms, condensed molecules, periodic optical potentials, an external trapping potential, and a Feshbach coupling term between atoms and molecules:

$$\hat{H} = \hat{\psi}^\dagger \left[\frac{\vec{p}^2}{2m_A} + V^A_{\text{trap}}(x,y,z) + V^{A1}_{\text{OL}}(t)\cos^2(kz) + V^{A2}_{\text{OL}}(t)\cos^2(2kz) \right] \hat{\psi} + \frac{4\pi\hbar^2 a_{AA}}{m_A} \hat{\psi}^\dagger \hat{\psi}^\dagger \hat{\psi}\hat{\psi},$$

$$+ \hat{\phi}^\dagger \left[\frac{\vec{p}^2}{2(2m_A)} + V^M_{\text{trap}}(x,y,z) + V^{M1}_{\text{OL}}(t)\cos^2(kz) + V^{M2}_{\text{OL}}(t)\cos^2(2kz) \right] \hat{\phi} + \frac{4\pi\hbar^2 a_{MM}}{2m_A} \hat{\phi}^\dagger \hat{\phi}^\dagger \hat{\phi}\hat{\phi}$$

$$+ \frac{4\pi\hbar^2 a_{AM}}{\mu} \hat{\psi}^\dagger \hat{\phi}^\dagger \hat{\psi}\hat{\phi} + g_{3D}(\hat{\phi}^\dagger \hat{\psi}\hat{\psi} + \hat{\psi}^\dagger \hat{\psi}^\dagger \hat{\phi}). \quad (1)$$

Here $\hat{\psi}$ is the atom field operator, $\hat{\phi}$ is the molecule field operator, m_A is the atomic mass, V^A_{trap} and V^M_{trap} are the trap potentials for the atoms and molecules that include the deep 2D optical lattice that traps the BECs (so that the atomic and molecular BECs are effectively 1D), the external magnetic-field potentials that are used to tune the relative energies of the atom and molecular BECs (and so also the Feshbach resonance), and the 1D optical lattice potentials V^{A1}_{OL}, V^{A2}_{OL}, V^{M1}_{OL}, V^{M2}_{OL} for the atoms and molecules due to the optical fields at wave vectors k and $2k$, and the potentials that modulate the dynamics of the BECs in the remaining nontrivial dimension, creating an effective band gap. The parameter g_{3D} is the Feshbach coupling coefficient.

If there are sufficient atoms and dimers in the BECs, the dynamics are well described by simplest level of description consisting of a mean-field approximation, and are given by the Gross-Pitaevskii (alias nonlinear Schrödinger) equations for the atom and molecule order parameters ψ and ϕ,

$$i\hbar\frac{\partial}{\partial t}\psi(t,x,y,z) = \left[-\frac{\hbar^2\Delta}{2m_A} + V^A_{\text{trap}}(x,y,z) + V^{A1}_{\text{OL}}(t)\cos^2(kz) + V^{A2}_{\text{OL}}(t)\cos^2(2kz) \right]\psi + \frac{4\pi\hbar^2 a_{AA}}{m_A} 2|\psi|^2\psi + \frac{4\pi\hbar^2 a_{AM}}{\mu}|\phi|^2\psi + 2g_{3D}\psi^*\phi, \quad (2a)$$

$$i\hbar\frac{\partial}{\partial t}\phi(t,x,y,z) = \left[-\frac{\hbar^2\Delta}{2(2m_A)} + V^M_{\text{trap}}(x,y,z) + V^{M1}_{\text{OL}}(t)\cos^2(kz) + V^{M2}_{\text{OL}}(t)\cos^2(2kz) \right]\phi + \frac{4\pi\hbar^2 a_{MM}}{2m_A} 2|\phi|^2\phi + \frac{4\pi\hbar^2 a_{AM}}{\mu}|\psi|^2\phi + g_{3D}\psi^2. \quad (2b)$$

An effectively 1D gas can be produced by applying a strong 2D optical lattice, which confines the 3D gas in two of its dimensions, forming an array of cigar-shaped clouds. If the radial confinement energy $\hbar\omega_\perp$ is large compared to other relevant energies in the system ("tight confinement"), atoms are restricted to move only in the direction of the cigars (the z axis) [20]. The system's dynamics are effectively 1D. With no radial excitations for tight confinement, the transverse cross section is constant. We can integrate over the radial coordinates to reduce the governing equations to 1+1 nontrivial dimensions [16,32–34]. The effective 1D scattering lengths, α_{AA}, α_{AM}, and α_{MM}, which describe the atom-atom, atom-molecule, and molecule-molecule interaction strengths, respectively, are functions of the 3D s-wave

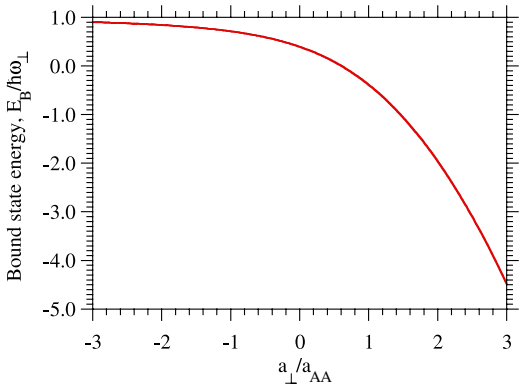

FIG. 1. (Color online) Quasi-1D Feshbach bound-state energy vs $a_{A\perp}/a_{AA}$ in a 2D confining harmonic potential.

scattering lengths, a_{AA}, a_{AM}, and a_{MM} (which themselves depend on the magnetic field), and the transverse harmonic lengths $a_{A\perp}=\sqrt{\hbar/m_A\omega_\perp}$, $a_{M\perp}=\sqrt{\hbar/m_M\omega_\perp}$. The 1D Feshbach coupling coefficient g_{1D} can be obtained similarly from the 3D Feshbach coefficient g_{3D} (defined below) and the transverse lengths. For example, the 1D atom-atom interaction strength takes the form [16,32]

$$\alpha_{AA}=\frac{2\hbar^2 a_{AA}}{ma_\perp^2}\left(1-\frac{a_{AA}}{a_\perp}\zeta(1/2)\right)^{-1}, \tag{3}$$

where $\zeta(\cdot)$ is the Riemann zeta function [35]. Confinement-induced resonances can result in this 1D limit when the denominator in Eq. (3) becomes large: The 1D scattering length α_{AA} diverges when the 3D scattering length takes the value $a_{AA}/a_{A\perp}=1/\zeta(1/2)\approx 0.6848$. The hard-core Tonks-Girardeau gas regime is accessed in this regime for $a_{AA}\gg n_{1D}(a_{A\perp})^2$, where n_{1D} is the maximum atom density.

For strong confinement, the two-body bound state has dimensionless binding energy $\mathcal{E}_B$, which depends on the bound-state energy E_B and the confining frequency $\omega_\perp$ according to

$$\mathcal{E}_B=(\hbar\omega_\perp-E_B)/2\hbar\omega_\perp=(\kappa_B a_{A\perp}/2)^2, \tag{4a}$$

where κ_B is the inverse longitudinal size of the dimer, which is determined by the condition [16,32],

$$\zeta(1/2,\mathcal{E}_B)+a_{A\perp}/a_{AA}=0, \tag{4b}$$

where the Hurvitz zeta function $\zeta(1/2,\mathcal{E})$ may be expressed as an integral [36],

$$\zeta(1/2,\mathcal{E})=\int_0^\infty \frac{dt}{\sqrt{\pi t}}\left(\frac{e^{-\mathcal{E}t}}{1-e^{-t}}-\frac{1}{t}\right). \tag{4c}$$

Since $\zeta(1/2,\mathcal{E})$ is monotonic in $\mathcal{E}$, there is precisely one such bound state for any given $a_{A\perp}/a_{AA}$. Figure 1 shows the bound-state energy E_B as a function of $a_{A\perp}/a_{AA}$. As long as $E_B<\hbar\omega_\perp$, there is a bound state. The figure shows that even for $a_{AA}<0$ (the BCS side of resonance for the fermion atom case), there is a confinement-induced resonance bound state.

More quantitatively, for tight confinement, the transverse (x,y) and longitudinal (z,t) dimensions can be separated, $\psi(t,x,y,z)=\psi(t,z)\psi_{\perp,A}(x,y)$, $\phi(t,x,y,z)=\phi(t,z)\phi_{\perp,A}(x,y)$. Then integration over the transverse coordinates leaves the nontrivial dynamics in the 1+1 dimensions of the longitudinal coordinates, with mean-field equations having modified coupling constants [16,32–34]

$$i\hbar\frac{\partial}{\partial t}\psi(t,z)=\left[-\frac{\hbar^2}{2m_A}\frac{\partial^2}{\partial z^2}+V_{\text{trap}}^{A0}+V_{\text{OL}}^{A1}(t)\cos^2(kz)+V_{\text{OL}}^{A2}(t)\cos^2(2kz)\right]\psi \tag{5a}$$

$$+\frac{4\pi\hbar^2\alpha_{AA}}{m_A}2|\psi|^2\psi+\frac{4\pi\hbar^2\alpha_{AM}}{\mu}|\phi|^2\psi+2g_{1D}\psi^*\phi, \tag{5b}$$

$$i\hbar\frac{\partial}{\partial t}\phi(t,z)=\left[-\frac{\hbar^2}{2(2m_A)}\frac{\partial^2}{\partial z^2}+V_{\text{trap}}^{M0}+V_{\text{OL}}^{M1}(t)\cos^2(kz)+V_{\text{OL}}^{M2}(t)\cos^2(2kz)\right]\phi \tag{5c}$$

$$+\frac{4\pi\hbar^2\alpha_{MM}}{2m_A}2|\phi|^2\phi+\frac{4\pi\hbar^2\alpha_{AM}}{\mu}|\psi|^2\phi+g_{1D}\psi^2. \tag{5d}$$

Suppose the atomic BEC order parameter ψ has components in the vicinity of wave numbers $\pm k$ and energy $\hbar\omega_1=\hbar^2k^2/(2m_A)$. And suppose, since we wish to treat atoms and molecules which are coupled by the Feshbach resonance, that the dimer BEC ϕ goes as the square of the atomic BEC, with wave numbers near $\pm 2k$ and frequencies (energies divided by $\hbar$) near $2\omega_1$. The dynamics may be then expressed in terms of slowly varying envelopes (SVEs), $\psi_+(t,z)$, $\psi_-(t,z)$, $\phi_+(t,z)$, $\phi_-(t,z)$, about carrier waves with those wave numbers and frequencies [37]. We assign SVEs about carrier waves with positive wave numbers the subscript plus ("+"), and SVEs about carrier waves with negative wave the subscript minus ("−"),

$$\psi(t,z)=\psi_+(t,z)\exp(-i\omega_1 t+ikz)+\psi_-(t,z)\exp(-i\omega_1 t-ikz), \tag{6a}$$

$$\phi(t,z)=\phi_+(t,z)\exp(-2i\omega_1 t+2ikz)+\phi_-(t,z)\times\exp(-2i\omega_1 t-2ikz). \tag{6b}$$

We insert Eq. (6) into the general governing Eqs. (5), and then separate out the parts of the equation in the relevant frequency bands. The SVEs obey a set of equations which are lengthier than the more general equations (5), but which are qualitatively simpler, since the SVEs contain only narrow energy and momentum component spreads:

$$i\hbar\psi_{+,t} = -i\frac{\hbar^2 k}{m_A}\psi_{+,z} - \frac{\hbar^2}{m_A}\psi_{+,zz} + \left(V_{\text{trap}}^{A0} + \frac{V_{OL}^{A1} + V_{OL}^{A2}}{2}\right)\psi_+ + \frac{V_{OL}^{A1}}{4}\psi_- + \frac{4\pi\hbar^2\alpha_{AA}}{m_A/2}\left[|\psi_+|^2 + 2|\psi_-|^2 + \frac{a_{MA}}{\alpha_{AA}}\frac{m_A/2}{\mu}(|\phi_+|^2 + |\phi_-|^2)\right]\psi_+ + 2g_{1D}\psi_+^*\phi_+, \quad (7a)$$

$$i\hbar\psi_{-,t} = i\frac{\hbar^2 k}{m_A}\psi_{-,z} - \frac{\hbar^2}{m_A}\psi_{-,zz} + \left(V_{\text{trap}}^{A0} + \frac{V_{OL}^{A1} + V_{OL}^{A2}}{2}\right)\psi_- + \frac{V_{OL}^{A1}}{4}\psi_+ + \frac{4\pi\hbar^2\alpha_{AA}}{m_A/2}\left[2|\psi_+|^2 + |\psi_-|^2 + \frac{a_{MA}}{\alpha_{AA}}\frac{m_A/2}{\mu}(|\phi_+|^2 + |\phi_-|^2)\right]\psi_- + 2g_{1D}\psi_-^*\phi_-, \quad (7b)$$

$$i\hbar\phi_{+,t} = -i\frac{\hbar^2 k}{2m_A}\phi_{+,z} - \frac{\hbar^2}{2m_A}\phi_{+,zz} + \left(V_{\text{trap}}^{M0} + \frac{V_{OL}^{M1} + V_{OL}^{M2}}{2}\right)\phi_+ + \frac{V_{OL}^{M2}}{4}\phi_- + \frac{4\pi\hbar^2\alpha_{MM}}{m_A}\left[\frac{a_{MA}}{\alpha_{MM}}\frac{m_A}{\mu}(|\psi_+|^2 + |\psi_-|^2) + |\phi_+|^2 + 2|\phi_-|^2\right]\phi_+ + g_{1D}\psi_+^2, \quad (7c)$$

$$i\hbar\phi_{-,t} = i\frac{\hbar^2 k}{2m_A}\phi_{-,z} - \frac{\hbar^2}{2m_A}\phi_{-,zz} + \left(V_{\text{trap}}^{M0} + \frac{V_{OL}^{M1} + V_{OL}^{M2}}{2}\right)\phi_- + \frac{V_{OL}^{M2}}{4}\phi_+ + \frac{4\pi\hbar^2\alpha_{MM}}{m_A}\left[\frac{a_{MA}}{\alpha_{MM}}\frac{m_A}{\mu}(|\psi_+|^2 + |\psi_-|^2) + 2|\phi_+|^2 + |\phi_-|^2\right]\phi_- + g_{1D}\psi_-^2. \quad (7d)$$

Here t and z are time and distance, subscripts t and z after a comma stand for partial derivatives, and an asterisk means complex conjugation. Equations (7a) and (7b) govern the evolution of $\psi_\pm$, which are SVEs of the atomic BEC centered about carrier waves with frequency ω_1 and wave vectors $\pm k_1$ (i.e., forward- and backward-moving SVEs). Equations (7c) and (7d) are for $\phi_\pm$, which are SVEs of the dimer BEC centered about carrier waves with frequency $2\omega_1$ and wave vectors $\pm 2k$ (they are forward- and backward-moving SVEs). The dispersion due to the optical lattice (first derivative terms in z together with linear coupling between the forward- and backward-moving SVEs) can be much stronger than the dispersion that is due to the kinetic energy terms (second derivatives in z), in which case the terms with second derivatives in z may be neglected. A dc magnetic field contributes different energies to the atom and dimer fields and this results in a detuning of the energy of the molecules relative to the energy of the atoms. We will see that the difference in the lowest-order components of the trap plus lattice also contributes to the detuning. We may therefore fold the effects of the flat magnetostatic field into the variables V_{trap}^{A0} and V_{trap}^{M0}. The system of equations (7) can also describe propagation of light in a nonlinear waveguide, with the variables representing different physical quantities [33,38]; since the BEC and optical cases are described by the same equations, they exhibit the same behavior.

It is helpful to rescale the governing equations (7) as follows:

$$\psi_+ \equiv \psi_+\sqrt{\frac{16\pi\hbar^2\alpha_{AA}}{V_{OL}^{A1}(m_A/2)}}\exp\{i[\omega_1' + (V_{\text{trap}}^{A0} + V_{OL}^{A1}/2 + V_{OL}^{A2}/2)/\hbar]t\}, \quad (8a)$$

$$\psi_- \equiv \psi_-\sqrt{\frac{16\pi\hbar^2\alpha_{AA}}{V_{OL}^{A1}(m_A/2)}}\exp\{i[\omega_1' + (V_{\text{trap}}^{A0} + V_{OL}^{A1}/2 + V_{OL}^{A2}/2)/\hbar]t\}, \quad (8b)$$

$$\phi_+ \equiv \phi_+\sqrt{\frac{16\pi\hbar^2\alpha_{AA}}{V_{OL}^{A1}(m_A/2)}}\exp\{i[2\omega_1' + (V_{\text{trap}}^{A0} + V_{OL}^{A1}/2 + V_{OL}^{A2}/2)/\hbar]t\}, \quad (8c)$$

$$\phi_- \equiv \phi_-\sqrt{\frac{16\pi\hbar^2\alpha_{AA}}{V_{OL}^{A1}(m_A/2)}}\exp\{i[2\omega_1' + (V_{\text{trap}}^{A0} + V_{OL}^{A1}/2 + V_{OL}^{A2}/2)/\hbar]t\}, \quad (8d)$$

$$\tau \equiv \frac{4\hbar}{V_{OL}^{A1}}t, \quad (8e)$$

$$\zeta \equiv \frac{4\hbar^2 k}{V_{OL}^{A1}m_a}z. \quad (8f)$$

Here we choose $\omega_1' = (V_{\text{trap}}^{A0} + V_{OL}^{A1}/2 + V_{OL}^{A2}/2)/\hbar$ as the frequency of the carrier wave of the atom SVEs and half the frequency of the carrier wave of the dimer SVEs. This yields normalized coupled-mode equations,

$$0 = -i\psi_{+,\tau} - i\psi_{+,\zeta} + \psi_- + \left[|\psi_+|^2 + 2|\psi_-|^2 + \frac{3\alpha_{AM}}{4\alpha_{AA}}(|\phi_+|^2 + |\phi_-|^2)\right]\psi_+ + 2\hat{g}\psi_+^*\phi_+, \quad (9a)$$

$$0 = -i\psi_{-,\tau} + i\psi_{-,\zeta} + \psi_+ + \left[2|\psi_+|^2 + |\psi_-|^2 + \frac{3\alpha_{AM}}{4\alpha_{AA}}(|\phi_+|^2 + |\phi_-|^2)\right]\psi_- + 2\hat{g}\psi_-^*\phi_-, \quad (9b)$$

$$0 = -i\phi_{+,\tau} - \frac{i}{2}\phi_{+,\zeta} + \Delta\phi_+ + \kappa\phi_- + \left[\frac{3\alpha_{AM}}{4\alpha_{AA}}(|\psi_+|^2 + |\psi_-|^2) + \frac{\alpha_{MM}}{2\alpha_{AA}}(|\phi_+|^2 + 2|\phi_-|^2)\right]\phi_+ + \hat{g}\psi_+^2, \quad (9c)$$

$$0 = -i\phi_{-,\tau} + \frac{i}{2}\phi_{-,\xi} + \Delta\phi_- + \kappa\phi_+ + \left[\frac{3\alpha_{AM}}{4\alpha_{AA}}(|\psi_+|^2 + |\psi_-|^2) + \frac{\alpha_{MM}}{2\alpha_{AA}}(2|\phi_+|^2 + |\phi_-|^2)\right]\phi_- + \hat{g}\psi_-^2, \tag{9d}$$

with dimensionless coefficients

$$\Delta = \frac{4}{V_{OL}^{A1}}\left[\left(V_{\text{trap}}^{M0} + \frac{V_{OL}^{M1} + V_{OL}^{M2}}{2}\right) - \left(V_{\text{trap}}^{A0} + \frac{V_{OL}^{A1} + V_{OL}^{A2}}{2}\right) - 2\hbar\omega_1'\right] \quad \text{(detuning)}, \tag{10a}$$

$$\kappa = \frac{V_{OL}^{M1}}{V_{OL}^{A1}} \quad \text{(Bragg coefficient)}, \tag{10b}$$

$$\hat{g} = \sqrt{\frac{V_{OL}^{A1}(m_A/2)}{16\pi\hbar^2\alpha_{AA}}}g \quad \text{(Feshbach coefficient)}. \tag{10c}$$

Many of the dimensionless parameters in Eqs. (9) are, in practice, adjustable; however, there are insufficient independent experimental variables to adjust all of the dimensionless parameters. The experimental parameters that can be varied are the components of the optical lattice at spatial frequencies k and $2k$ (in phase with the atom and dimer BECs, respectively), the spatially flat dc magnetic-field strength, and the strength of the 2D optical lattice that confined the BECs to 1D cigar shapes. In the resulting dynamics, the detuning Δ acts to change the frequency difference between the atoms and dimers, and this parameter can be changed as a function of time by tuning the external magnetic field. κ expresses the ratio of the strength of the Bragg scattering—forward-moving light being bounced backwards by the optical lattice, and vice versa—of the molecules compared to the atoms (in which the Bragg scattering coefficient is normalized to unity). $\hat{g}$ is a Feshbach term, which causes atoms to bind and form molecules and causes dimers to interact with atoms and split up. The nonlinearities are normalized such that the atom's self-mean-field coefficient is unity; $\hat{g}$ represents the ratio of the Feshbach to self-mean-field coefficients.

III. GAP SOLITONS

We find solutions using the relaxation method [39]. Consider eigenvector solutions having a given energy. For this system, that means $\psi_+(t,z)=\exp(-i\omega t)\psi_+(z)$, $\psi_-(t,z)=\exp(-i\omega t)\psi_-(z)$, $\phi_+(t,z)=\exp(-2i\omega t)\phi_+(z)$, $\phi_-(t,z)=\exp(-2i\omega t)\phi_-(z)$. Hence the time derivatives in the dynamical equations (9) can be turned into multiplication by constants. Next, the spatial axis is discretized, changing the derivatives in space to differences. The system is then a set of algebraic difference equations, rather than partial differential equations. The algebraic equations are solved using Newton's method. Since the equations are nonlinear, there is no fully automatic way to find a complete set of possible solutions—one must use inferences and guesses. We begin with solutions to known limits, and then evolve the system by small increments, using one solution as the initial guess in Newton's method for the next value. By thus gradually evolving the solutions, we build up a description of the solutions over a finite multidimensional section of the parameter space.

In the absence of Feshbach resonances ($\hat{g}=0$), the equations support (well-known) gap soliton solutions. The quiescent (zero-velocity) gap solitons of atoms take the form [28,29]

$$\psi_+(z,t) = \frac{\sin Q}{\sqrt{3}}\,\text{sech}(z\sin Q - iQ/2)\exp[-i\cos(Q)t], \tag{11a}$$

$$\psi_-(z,t) = -\frac{\sin Q}{\sqrt{3}}\,\text{sech}(z\sin Q + iQ/2)\exp[-i\cos(Q)t]. \tag{11b}$$

With (or without) a nonzero Feshbach resonance ($g,\hat{g}\neq 0$), there are gap solitons (we will refer to all solitary wave solutions as solitons, regardless of stability) with essentially the same shape as the gap soliton of atoms, but scaled differently,

$$\phi_+(z,t) = \sqrt{\frac{\kappa}{3\chi_{\text{spm}}}}\sin Q\,\text{sech}(2\kappa z\sin Q - iQ/2) \times\exp[-i(\Delta+\cos Q)\kappa t], \tag{12a}$$

$$\phi_-(z,t) = -\sqrt{\frac{\kappa}{3\chi_{\text{spm}}}}\sin Q\,\text{sech}(2\kappa z\sin Q + iQ/2) \times\exp[-i(\Delta+\cos Q)\kappa t], \tag{12b}$$

where $\chi_{\text{spm}}=\alpha_{MM}/(2\alpha_{AA})$ is the coefficient of self-mean-field in Eqs. (9c) and (9d). The variable Q, which takes values $0<Q<\pi$, parametrizes the entire family of gap soliton solutions—width, amplitude, frequency, phase, etc. There are also known families of solitons in systems that have Feshbach-like terms and that lack self- and cross-mean-field nonlinearities [30]. Our numerical simulations took as starting points the solutions for the equations with mean-field and without Feshbach terms (rather than vice versa). We illustrate the two type of solutions by showing all the complex-valued solutions of each of the components. Figure 2 is a gap soliton with dimers only, and Fig. 3 is a gap soliton with both atomic and dimer BECs.

For the direct numerical simulations herein, we arbitrarily take the ratios of scattering lengths as follows: $a_{AM}=1.09a_{AA}$ and $\alpha MM/\alpha_{AA}$, independent of the magnetostatic field.

To illustrate the behavior, we give two planar cross sections of the higher-dimensional parameter space. Figure 4 shows that for a particular set of coefficients, gap solitons with both atoms and molecules exist only if the gap for the molecular BEC is larger than the gap of the atom BEC—the strength of the OL component at higher spatial frequency, in

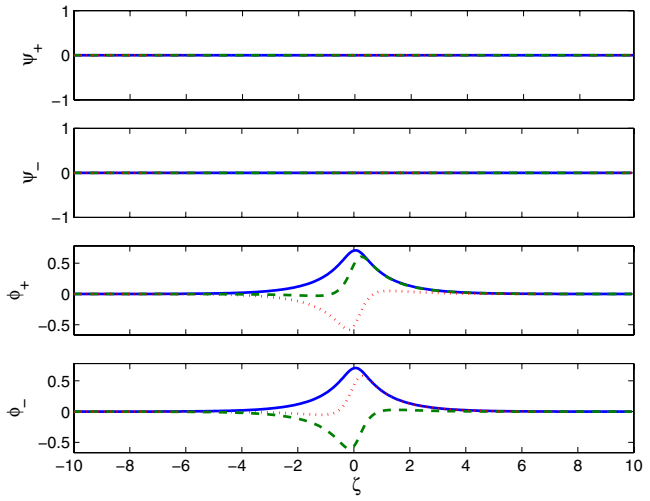

FIG. 2. (Color online) Gap soliton with zero atomic BEC and nonzero dimer BEC. Solid curves represent the magnitude of the order parameters, dashed and dotted curves are the real and imaginary parts of the order parameters.

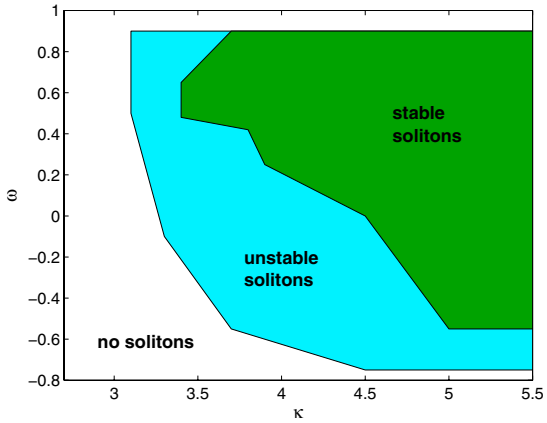

FIG. 4. (Color online) Existence and stability regions of quiescent gap solitons in parameter space of frequency ω and relative OL strength parameter κ, holding other parameters constant—detuning coefficient $\Delta=0.8$, nonlinear coefficients $\alpha_{AA}=-2$, $\alpha_{AM}/\alpha_{AA}=0.82$, $\alpha_{MM}/\alpha_{AA}=1.22$ and dimensionless Feshbach coefficient $\hat{g}/\alpha_{AA}=0.5$.

phase with the molecular BEC, must be at least about three times stronger than the component of the OL at lower spatial frequency, in phase with the atom BEC.

Figure 5 shows the existence and stability of gap solitons over a slice of the parameter space ω-Δ in energy and detuning. It is likely that the very top region (near $\omega=1$) is stable and the "instability" shown in the figure is a numerical artifact due to the finite grid size.

When gap solitons are moving ($\mathcal{V}\neq 0$) they have different shapes and stability properties than quiescent ($\mathcal{V}=0$) gap solitons. For example, Fig. 6 shows that for gap solitons with both atoms and molecules, at a given set of parameter values—detuning, Feshbach, and Kerr coefficients—the faster the gap solitons are moving, the smaller is the percentage of the gap in which there exist soliton solutions. At approximately half the maximum velocity, this type of gap soliton does not exist at all. There are fewer gap solitons at frequencies in the lower half of the band gap than in the upper half, with the most soliton solutions twice as close to the top of the band gap as to the bottom of the gap. The solitons are stable in the region of low velocity, but lose their stability with increased velocity. In the region of negative frequencies, solitons are unstable at lower velocities then solitons with positive frequencies. Soliton mass (or the number of atoms in the soliton) decreases with growth of (the absolute value of the) velocity, especially the components moving opposite to the direction of propagation—the symmetry about the center of the soliton is broken at nonzero velocity. Figure 7 shows a stable soliton, and Fig. 8 shows an unstable soliton.

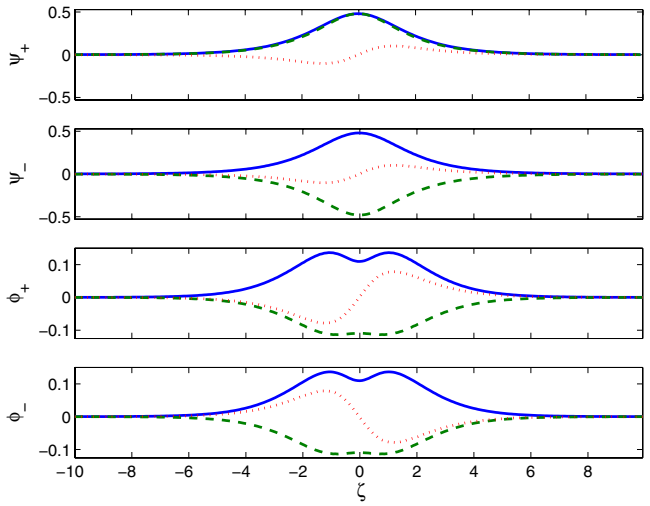

FIG. 3. (Color online) Gap soliton with nonzero atomic and dimer BECs. Solid curves represent the magnitude of the order parameters, dashed and dotted curves are the real and imaginary parts of the order parameters.

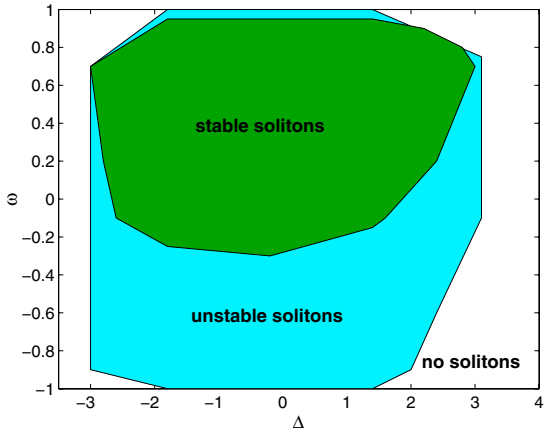

FIG. 5. (Color online) Existence and stability regions of quiescent gap solitons in parameter space of frequency ω and detuning Δ, holding other parameters constant—Bragg coupling coefficient $\kappa=5$, nonlinear coefficients $\alpha_{AA}=-2$, $0.75\alpha_{AM}/\alpha_{AA}=0.82$, $\alpha_{MM}/\alpha_{AA}=1.22$, and dimensionless Feshbach coefficient $\hat{g}/\alpha_{AA}=0.5$.

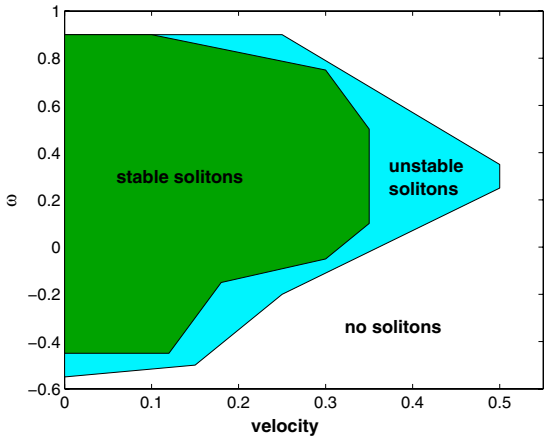

FIG. 6. (Color online) Existence and stability regions of moving gap solitons in parameter space of frequency ω and velocity $\mathcal{V}$, holding the rest of the parameters constant at dimensionless detuning $\Delta=0.6$, Bragg coupling coefficient $\kappa=5$, nonlinear coefficients $\alpha_{AA}=-2$, $0.75\alpha_{AM}/\alpha_{AA}=0.82$, $\alpha_{MM}/\alpha_{AA}=1.22$, and dimensionless Feshbach coefficient $\hat{g}/\alpha_{AA}=0.5$.

IV. DYNAMICAL PREPARATION OF DIMER GAP SOLITONS FROM AN ATOMIC BEC

We predict that pure dimer gap solitons can be obtained starting from a BEC of atoms only. The two families of gap solitons—one with a mix of both atom and dimer BECs, the other with dimers only—are distinct, and we do not know how to transform one into the other adiabatically. Instead, we give a nonadiabatic route from an atom BEC to a dimer gap soliton. We begin with a BEC of atoms, in a system with a very large detuning between atoms and molecules. Although at any given point in time, the Feshbach resonance causes some of the atoms to bind with one another (become dimer molecules), the large detuning ensures that the molecular BEC field does not accumulate. Hence we start with an approximation of the exact gap soliton [Eqs. (11)] for the system (9) with zero Feshbach ($\hat{g}=0$), atoms only. These are, mathematically, the standard gap solitons [28]. In our direct simulations of the equations (using a split-step fast Fourier transform scheme [33]), we do not take the initial conditions to be the exact gap solitons (11), which are hyperbolic secants. Rather, since Gaussians are likelier to be available in experiment, we take as initial conditions Gaussians, with the correct initial phases imprinted on the BEC by a short optical potential [40],

$$\psi_+^G(z,t=0)=A_G\exp[-(z/W_G)^2+ik_Gz], \tag{13a}$$

$$\psi_-^G(z,t=0)=-A_G\exp[-(z/W_G)^2-ik_Gz]. \tag{13b}$$

The coefficients that give the Gaussian the same mass (number of atoms in the condensate), maximum density, and wave numbers as the exact (hyperbolic secant) solution are

$$A_G=\sqrt{\frac{2}{3}(1-\cos Q)}, \tag{14a}$$

$$W_G=\pi^{-1/2}\frac{Q}{1-\cos Q}, \tag{14b}$$

$$k_G=1-\cos Q, \tag{14c}$$

where Q is the same parameter as in the exact expression (11) for the gap soliton of atoms. This is not exactly an eigenstate, but it is very close and almost all of the BEC has frequency $\omega=\cos Q$. Also, note that for dimers, the Gaussian parameters that fit the exact gap soliton solution (12) are similar but scaled,

$$A_G=\sqrt{\frac{\kappa}{\chi_{\rm spm}}\frac{2}{3}(1-\cos Q)}, \tag{15a}$$

$$W_G=\frac{\pi^{-1/2}}{2\kappa}\frac{Q}{1-\cos Q}, \tag{15b}$$

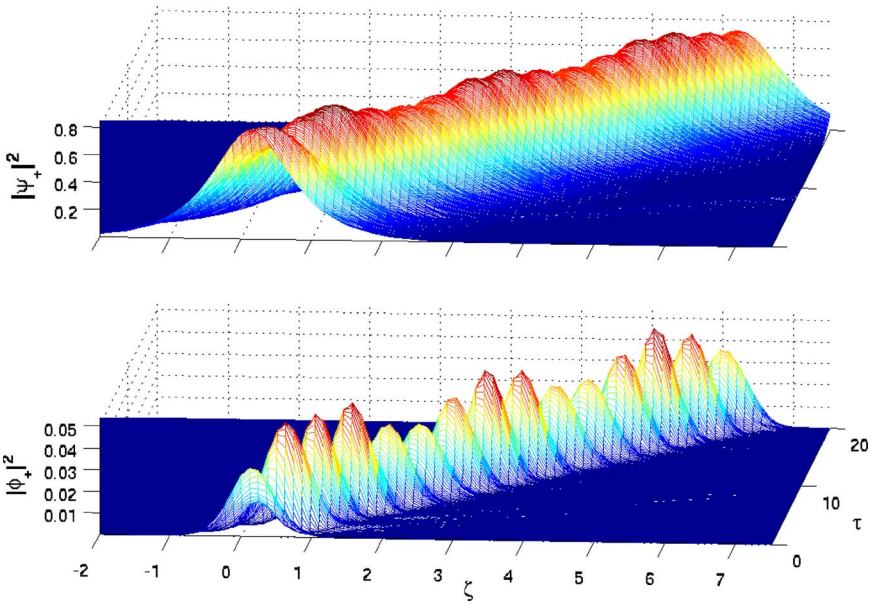

FIG. 7. (Color online) Propagation of a stable moving solitary wave ($\omega=0.3$, $\mathcal{V}=0.3$).

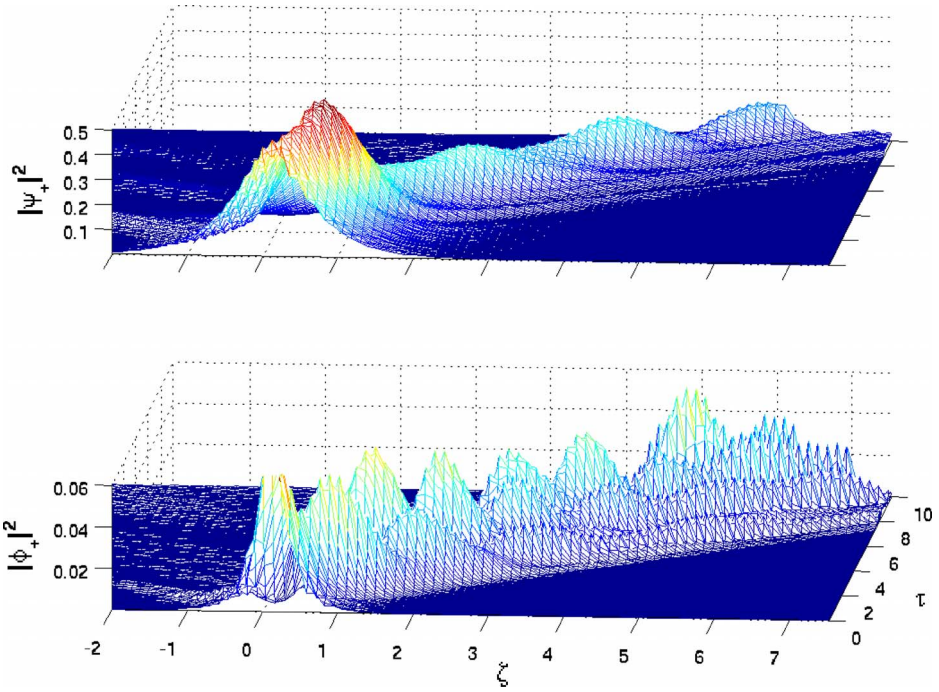

FIG. 8. (Color online) Propagation of an unstable moving solitary wave ($\omega=-0.2$, $\mathcal{V}=0.2$).

$$k_G = \frac{1-\cos Q}{2\kappa}, \tag{15c}$$

where κ is the Bragg coefficient and $\chi_{\rm spm}=\alpha_{MM}/(2\alpha_{AA})$ is the self-mean-field coefficient (i.e., the self-phase modulation coefficient in the nonlinear optics context) in Eqs. (9c) and (9d). The detuning was then, by altering the dc magnetic field, abruptly changed to zero. The dimer BEC then started to grow, and the growth *was not* washed out by a quickly varying phase. In our simulations, we kept the OL component in-phase with the dimers at zero (i.e., off) during this stage (though having it nonzero is a degree of freedom that may be employed to optimize the evolution). After a finite time, we *turned off* the OL component in-phase with the atom BEC, and we *turned on* the OL component in-phase with the dimer BEC. We also changed the dc magnetic field such that the atoms and molecules were strongly detuned. We made an additional adjustment to the self- and cross-mean-field terms via the confining OL. The OL lattices are chosen such that the linear and nonlinear coefficients are those that make the existing dimer field approximately a gap soliton,

$$Q = \frac{kM}{2|A_{\rm max}|^2}, \tag{16a}$$

$$\kappa = \frac{k/2}{1-\cos Q}, \tag{16b}$$

$$\chi_{\rm spm} = \frac{k}{3|A_{\rm max}|^2}, \tag{16c}$$

where $M=\int(|\phi_+|^2+|\phi_-|^2)dz$ is the area under the curve of the dimer BEC ("mass"), $|A_{\rm max}|^2$ is the average of the density maxima of the dimer BEC components in the forward- and backward-moving directions ("peak density"), and k is half the difference in wave numbers between the forward and backward modes ("relative wave vector"). When the shape of the dimer BEC is close enough to a Gaussian or hyperbolic secant, the nonlinearity and the dispersion caused by the OL hold the molecules in the form of a gap soliton, with just a small amount of excited modes due to the nonexact initial gap soliton conditions. At the same time, the OL component that is in-phase with the atoms is turned off, which lets the atoms escape to the left and to the right. For this scheme to work, the dimer BEC must be within the stable regime of the gap soliton, or roughly $Q \leqslant 1.01\pi/2$, otherwise, excitations will grow and eventually destroy the gap soliton. The process is illustrated in Fig. 9. We started out with an atomic BEC gap soliton (approximate, based on Gaussians). For one unit of dimensionless time, the detuning was reduced to zero, and from time equal to one the OL in phase with the atoms was turned off, the OL in phase with the dimers was turned on and the OL strengths were adjusted to give the dimers as a gap soliton. The result was a portion of the atom BEC converted to a gap soliton comprised of dimers, with some amount of extra energy, manifested in a small oscillation of the gap soliton, while the remainder of the atom field, which did not go into dimers, escaped either forward or backward.

So, by knowing the formulas connecting the parameters of a gap soliton pulse with the experimentally adjustable coefficients of the equation, we were able to allow the Feshbach term to cause a growth of a dimer BEC pulse. We identified where it the dimer pulse would be stable, and then changed the experimental parameters so that the system would capture (approximately) a stable gap soliton pulse comprised of a pure dimer BEC and allow excess atomic BEC to escape.

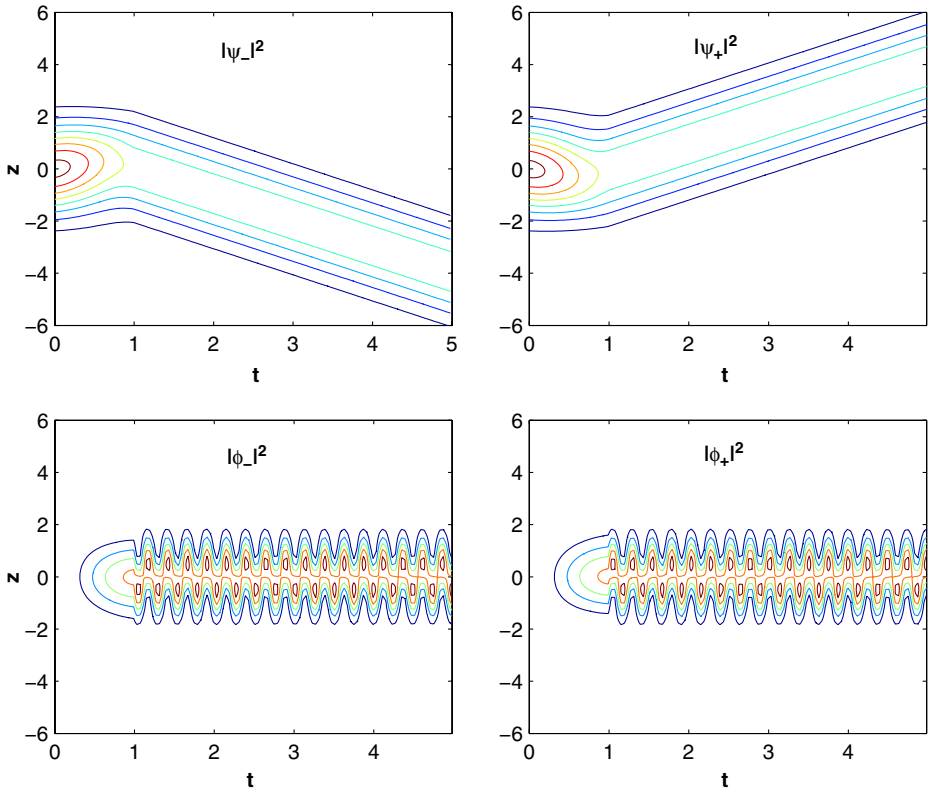

FIG. 9. (Color online) Evolution of an atomic BEC into a dimer BEC in the form of a gap soliton, and some atom BEC scattered away from the center. The top graphs are the atom BECs, and the bottom graphs are dimer BECs. The left graphs are the backward-moving BEC components, and the right graphs are the forward-moving BEC components. An initial atom BEC gap soliton with $\cos Q=0.75$, Feshbach coefficient $g=1$, and zero detuning $\Delta=0$ from dimensionless time from 0 to 1, and from time 1, the optical lattices release the atom BEC and trap the dimer BEC into a gap soliton plus a small perturbation. From dimensionless time 1, the OL component in-phase with the dimer BEC has Bragg coefficient $\kappa=0.42$. and the longitudinal, or trapping, OL is such that the self-mean-field coefficient of the dimer BEC is $\chi_{\mathrm{spm}}=4.3$.

V. SUMMARY AND CONCLUSION

We analyzed systems of Bose-Einstein condensates (BECs) confined to one dimension by a strong ("tight-binding") trapping two-dimensional optical lattice (OL), and with a weak OL perpendicular to it which creates a band gap. The BECs are subject to self- and cross-mean-field and a Feshbach term which couples atoms to dimer molecules. We derived coupled mode equations for the system, searched for solutions by a relaxation method [39], and analyzed the dynamics by direct numerical simulations using the split-step fast Fourier transform method [33].

We found that this system can support stable gap solitons comprised of atomic *and/or molecular* BECs. There are two distinct families of gap soliton solutions. One gap soliton solution, which is mathematically well known in the optics literature, has only a dimer BEC and no atom BEC. This limit is identical to that in Refs. [28]. The other family of soliton solutions is comprised of both atomic and dimer BECs, coupled together in position and in phase by the optical lattice, Feshbach resonance, and mean-field effects. We described these gap solitons in quantitative detail, delineating regions of stability and instability.

We also describe a procedure by which the system can start with an atomic BEC and produce a gap soliton composed *only* of a dimer BEC. This is done by starting with an atomic BEC pulse, suddenly adjusting the magnetostatic field such that the detuning is nearly zero ($\Delta=0$), and allowing the dimer BEC to grow. After a period of time, the OL component that causes Bragg scattering of the atom field is turned off; the OL component that causes Bragg scattering in the dimer BEC is adjusted, and the strength of the confining 2D optical lattice is adjusted, so that the dimer BEC pulse is approximately a gap soliton of the system. The atom BEC escapes forward and backward, and the molecular BEC remains in the center in the form of a gap soliton.

ACKNOWLEDGMENTS

This work was supported in part by grants from the U.S.-Israel Binational Science Foundation (Grant No. 2002147), the Israel Science Foundation for a Center of Excellence (Grant No. 8006/03), the German Federal Ministry of Education and Research (BMBF) through the DIP project, and the James Franck Program German-Israel Binational Program in Laser-Matter Interactions.

[1] H. Feshbach, Ann. Phys. (N.Y.) **19**, 287 (1962); *Theoretical Nuclear Physics* (Wiley, New York, 1992).

[2] E. Timmermans, P. Tommasini, M. Hussein, and A. Kerman, Phys. Rep. **315**, 199 (1999).

[3] M. Greiner, C. A. Regal, and D. Jin, Nature (London) **426**, 537 (2003); S. Jochim, M. Bartenstein, A. Altmeyer, G. Hendl, S. Riedl, C. Chin, J. H. Denschlag, and R. Grimm, Science **302**, 2101 (2003); S. Jochim, M. Bartenstein, A. Altmeyer, G.

Hendl, C. Chin, J. H. Denschlag, and R. Grimm, Phys. Rev. Lett. **91**, 240402 (2003); M. W. Zwierlein, C. A. Stan, C. H. Schunck, S. M. F. Raupach, S. Gupta, Z. Hadzibabic, and W. Ketterle, *ibid.* **91**, 250401 (2003); J. Cubizolles, T. Bourdel, S. J. J. M. F. Kokkelmans, G. V. Shlyapnikov, and C. Salomon, *ibid.* **91**, 240401 (2003); K. E. Strecker, G. B. Partridge, and R. G. Hulet, *ibid.* **91**, 080406 (2003); J. Kinast, S. L. Hemmer, M. E. Gehm, A. Turlapov, and J. E. Thomas, *ibid.* **92**, 150402 (2004).

[4] S. Inouye, M. R. Andrews, J. Stenger, H.-J. Miesner, D. M. Staper-Kurn, and W. Ketterle, Nature (London) **392**, 151 (1998).

[5] J. Stenger, S. Inouye, M. R. Andrews, H.-J. Miesner, D. M. Stamper-Kurn, and W. Ketterle, Phys. Rev. Lett. **82**, 2422 (1999).

[6] S. L. Cornish, N. R. Claussen, J. L. Roberts, E. A. Cornell, and C. E. Wieman, Phys. Rev. Lett. **85**, 1795 (2000).

[7] K. Xu, T. Mukaiyama, J. R. Abo-Shaeer, J. K. Chin, D. E. Miller, and W. Ketterle, Phys. Rev. Lett. **91**, 210402 (2003); T. Mukaiyama, J. R. Abo-Shaeer, K. Xu, J. K. Chin, and W. Ketterle, *ibid.* **92**, 180402 (2004); K. Xu, T. Mukaiyama, J. R. Abo-Shaeer, J. K. Chin, D. E. Miller, and W. Ketterle, *ibid.* **91**, 210402 (2003).

[8] J. Herbig, T. Kraemer, M. Mark, T. Weber, C. Chin, H.-C. Nagerl, and R. Grimm, Science **301**, 1510 (2003).

[9] M. Mark, T. Kraemer, J. Herbig, C. Chin, H.-C. Nagerl, and R. Grimm, Europhys. Lett. **69**, 706 (2005).

[10] S. Dürr, T. Volz, A. Marte, and G. Rempe, Phys. Rev. Lett. **92**, 020406 (2004).

[11] S. Dürr, T. Volz, and G. Rempe, Phys. Rev. A **70**, 031601(R) (2004).

[12] C. A. Regal, C. Ticknor, J. L. Bohn, and D. S. Jin, Nature (London) **424**, 47 (2003).

[13] M. Greiner, C. A. Regal, and D. Jin, Nature (London) **426**, 537 (2003).

[14] F. A. van Abeelen and B. J. Verhaar, Phys. Rev. Lett. **83**, 1550 (1999); F. H. Mies, E. Tiesinga, and P. S. Julienne, Phys. Rev. A **61**, 022721 (2000); V. A. Yurovsky and A. Ben-Reuven, *ibid.* **67**, 043611 (2003); J. P. D'Incao and B. D. Esry, Phys. Rev. Lett. **94**, 213201 (2005).

[15] D. S. Petrov, C. Salomon, and G. V. Shlyapnikov, Phys. Rev. Lett. **93**, 090404 (2004).

[16] M. Olshanii, Phys. Rev. Lett. **81**, 938 (1998).

[17] H. Moritz, T. Stoferle, K. Guenter, M. Kohl, and T. Esslinger, Phys. Rev. Lett. **94**, 210401 (2005).

[18] Y. A. Yurovsky and Y. B. Band, e-print physics/0602181.

[19] K. V. Kheruntsyan, D. M. Gangardt, P. D. Drummond, and G. V. Shlyapnikov, Phys. Rev. Lett. **91**, 040403 (2003).

[20] B. Laburthe Tolra, K. M. O'Hara, J. H. Huckans, W. D. Phillips, S. L. Rolston, and J. V. Porto, Phys. Rev. Lett. **92**, 190401 (2004).

[21] T. Rom, T. Best, O. Mandel, A. Widera, M. Greiner, T. W. Hansch, and I. Bloch, Phys. Rev. Lett. **93**, 073002 (2004).

[22] G. Thalhammer, K. Winkler, F. Lang, S. Schmid, R. Grimm, and J. H. Denschlag, Phys. Rev. Lett. **96**, 050402 (2006).

[23] T. Volz, N. Syassen, D. M. Bauer, E. Hansis, S. Dürr, and G. Rempe, Nat. Phys. **2**, 692 (2006).

[24] C. Ospelkaus, S. Ospelkaus, L. Humbert, P. Ernst, K. Sengstock, and K. Bongs, Phys. Rev. Lett. **97**, 120402 (2006).

[25] B. Damski, L. Santos, E. Tiemann, M. Lewenstein, S. Kotochigova, P. Julienne, and P. Zoller, Phys. Rev. Lett. **90**, 110401 (2003).

[26] E. A. Donley, N. R. Claussen, S. T. Thompson, and C. E. Wieman, Nature (London) **417**, 529 (2002).

[27] D. Jaksch, V. Venturi, J. I. Cirac, C. J. Williams, and P. Zoller, Phys. Rev. Lett. **89**, 040402 (2002).

[28] A. B. Aceves and S. Wabnitz, Phys. Lett. A **141**, 37 (1989); W. Chen and D. L. Mills, Phys. Rev. Lett. **58**, 160 (1987); D. N. Christodoulides and R. I. Joseph, *ibid.* **62**, 1746 (1989); R. F. Nabiev, P. Yeh, and D. Botez, Opt. Lett. **18**, 1612 (1993); J. Feng, *ibid.* **18**, 1302 (1993); C. M. de Sterke and J. E. Sipe, Prog. Opt. **33**, 203 (1994); Opt. Express **3**, 384 (1998); A. B. Aceves, Chaos **10**, 584 (2002).

[29] K. M. Hilligsøe, M. K. Oberthaler, and K.-P. Marzlin, Phys. Rev. A **66**, 063605 (2002); P. J. Y. Louis, E. A. Ostrovskaya, and Y. S. Kivshar, *ibid.* **71**, 023612 (2005); B. Eiermann, P. Treutlein, Th. Anker, M. Albiez, M. Taglieber, K.-P. Marzlin, and M. K. Oberthaler, Phys. Rev. Lett. **91**, 060402 (2003); L. Fallani, F. S. Cataliotti, J. Catani, C. Fort, M. Modugno, M. Zawada, and M. Inguscio, *ibid.* **91**, 240405 (2003); Th. Anker, M. Albiez, B. Eiermann, M. Taglieber, and M. K. Oberthaler, Opt. Express **12**, 11 (2004); H. Pu, L. O. Baksmaty, W. Zhang, N. P. Bigelow, and P. Meystre, Phys. Rev. A **67**, 043605 (2003); B. Eiermann, Th. Anker, M. Albiez, M. Taglieber, P. Treutlein, K.-P. Marzlin, and M. K. Oberthaler, Phys. Rev. Lett. **92**, 230401 (2004).

[30] T. Peschel, U. Peschel, F. Lederer, and B. A. Malomed, Phys. Rev. E **55**, 4730 (1997); C. Conti, S. Trillo, and G. Assanto, Opt. Express **3**, 389 (1998); Opt. Lett. **23**, 334 (1998).

[31] R. S. Tasgal, Y. B. Band, and B. A. Malomed, Phys. Rev. E **72**, 016624 (2005).

[32] T. Bergeman, M. G. Moore, and M. Olshanii, Phys. Rev. Lett. **91**, 163201 (2003).

[33] G. P. Agrawal, *Nonlinear Fiber Optics* (Academic, San Diego, 1989).

[34] Y. Kodama and A. Hasegawa, IEEE J. Quantum Electron. **QE-23**, 510 (1987).

[35] *Handbook of Mathematical Functions*, edited by M. Abramowitz and I. A. Stegun, 10th edition (Department of Commerce, Washington, D.C., 1972).

[36] C. Mora, R. Egger, and A. O. Gogolin, Phys. Rev. A **71**, 052705 (2005).

[37] Y. B. Band, M. Trippenbach, J. P. Burke, and P. S. Julienne, Phys. Rev. Lett. **84**, 5462 (2000); M. Trippenbach, Y. B. Band, and P. S. Julienne, Phys. Rev. A **62**, 023608 (2000); J. P. Burke, P. S. Julienne, C. J. Williams, Y. B. Band, and M. Trippenbach, *ibid.* **70**, 033606 (2004).

[38] R. Y. Chiao, E. Garmire, and C. H. Townes, Phys. Rev. Lett. **13**, 479 (1964).

[39] W. H. Press, S. A. Teukolsky, W. T. Vetterling, and B. P. Flannery, *Numerical Recipes in Fortran* (Cambridge University Press, Cambridge, England, 1992).

[40] L. Dobrek, M. Gajda, M. Lewenstein, K. Sengstock, G. Birkl, and W. Ertmer, Phys. Rev. A **60**, R3381 (1999); J. Denschlag *et al.*, Science **287**, 97 (2000); S. Burger, K. Bongs, S. Dettmer, W. Ertmer, K. Sengstock, A. Sanpera, G. V. Shlyapnikov, and M. Lewenstein, Phys. Rev. Lett. **83**, 5198 (1999).